Proceedings of the 3rd IEEE Int. Conf. on
Nano/Micro Engineered and Molecular Systems
January 6-9, 2008, Sanya, China

Formation of Gold Nano-particle Chains by DEP – a Parametric Experimental Analysis

Siu Ling Leung [1], Ming Lin Li [2] and Wen J. Li [1,2] *

[1] *Centre for Micro and Nano Systems, The Chinese University of Hong Kong, Hong Kong SAR, China.*
[2] *Micro and Nano Automation Laboratory, Shenyang Institute of Automation, Chinese Academy of Sciences, Shenyang, China*

Abstract— **Experimental results on varying particle size and dielectrophoretic (DEP) parameters, including voltage and frequency, are reported in this paper for investigating their effect on Au nano-particles Pearl Chain Formation (PCF). PCF was observed from 10kHz to 5MHz for 100nm gold Nano-particles (NPs), and 100kHz to 10MHz for 10nm gold NPs. Variations in formation rate were detected when the applied voltage and particle size varied. With higher voltage, pearl chain begins to form at higher rate and the formation time decreases. The optimum frequency of the gold NPs PCF shifts to higher frequency region when the particle size decreases. Theoretical analysis was carried out by applying the theories of DEP force and AC electrokinetics to explain the observations in the DEP frequency ranging from 10 Hz to 10MHz.**

Keywords — **AC electrokinetics, DEP Based Assembly, Dielectrophoresis Force, Gold Collodial Particles, Nano-assembly**

INTRODUCTION

Gold Nanoparticles (NPs) or colloidals have been extensively studied because of their potential applications in nanomedicine [1-2], nano-photonics [3] and nano devices [4]. In the past few decades, varieties of nanowire fabrication techniques have been developed. The most common methodology is the vapor-liquid-solid (VLS) synthesis method, which was first reported in 1964 by Wanger and Ellis [5]. However, secondary processes of VLS limit the usefulness of nanowire. Recently, dielectrophoretic (DEP) technique is becoming more popular to form nanowires because of its simplicity of implementation (e.g., see [6]).

DEP technique assembles nanowires in a single step, in which dielectric particles experience a force enhanced by non-uniform electric field as a result of polarization [7]. Despite numerous papers discussing the formation of gold pearl chain by DEP force, very few researchers explain the experimental results on the low- and high- frequency ranges, especially in regions which pearl chain cannot be formed.

This project is funded by the Chinese National 863 Plan (Project Code: 2007AA04Z317), National Natural Science Foundation of China (Project Code: 60675060), and Hong Kong Research Grants Council (Project Code: 413906)
*Contact Author: Wen J. Li (wen@mae.cuhk.edu.hk); Wen J. Li is a professor at The Chinese University of Hong Kong and also an affiliated professor at Shenyang Institute of Automation, CAS.

In this paper, we present a systematic study of Au NPs PCF together with an analysis of the dominant forces that induce the result.

ELECTRODE FABRICATION

Au electrodes with gap separation of 2 μm (Fig. 1) were fabricated on Si/SiO2 substrates by a lift-off process. Si wafers were first cleaned by immersing then in acetone, followed by IPA, and finally by DI-water. Then photoresist (AZ5214E) was spin-coated on the wafers at 3000rpm. The photoresist was then patterned by negative lithography. Finally, layers of 500Å chromium and 3000Å gold films were deposited on top of the patterned photoresist by thermal evaporation before lift-off. Gold colloidal solutions (EM. GC series from British Biocell International, Cardiff, U.K.) with 10 nm and 100 nm diameter particles were used in our experiments.

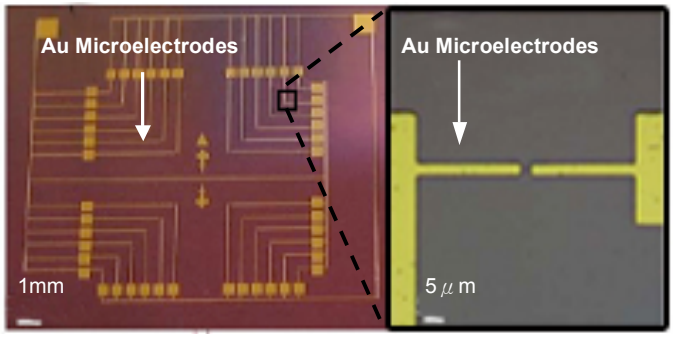

Figure 1. (a) Micro-photograph of Au microelectrodes fabricated on a Si substrate. (b) Optical image showing a pair of microelectrodes.

EXPERIMENTAL SETUP

The experimental setup was developed as shown in Fig. 2. A pulse/ Function Generator (Hp 811A, Hewlett Parkward Company, USA) was used to generate a sinusoidal A.C. current input for nanowire formation. A digital Real-Time Oscilloscope (TDS 220, Tektronix, Inc. USA) was used to measure the voltage change across Resistor A. Time was recorded by a stopwatch when the voltage change was observed. A resistor was used to prevent both the burnt out of electrodes due to heating and further growth of the formed nanowire (nano-particle chain).

Before the nanowire is formed, the circuit including the electrodes and the electric source can be considered to be an open one with infinity resistance due to the dielectric solution. The average resistance of gold nanowire is measured around 113.36Ω. Voltages across the electrodes and the Resistor A before and after nanowire formation were measured. At the beginning, voltages across the electrodes and the Resistor A were measured around $100mV_{pk\text{-}pk}$ and $11.9V_{pk\text{-}pk}$ when $12V_{pk\text{-}pk}$ voltage was applied to the circuit. Fig. 3 shows both experimentally measured and theoretically calculated (by Ohm's Law) voltages across the electrodes and the Resistor A after the formation of nanowire. According to the comparison in Fig. 3, Resistor A with 3kΩ was chosen for our circuit, such that more than 95% of the input voltage could be drawn by the resistor when a nanowire with ~100Ω resistance was formed.

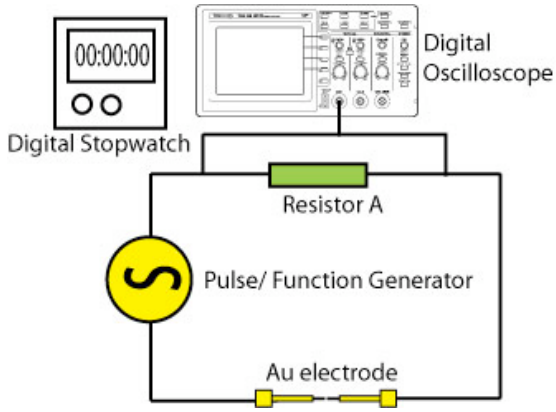

Figure 2. Schematic diagram of the experimental setup for nanowire formation detection.

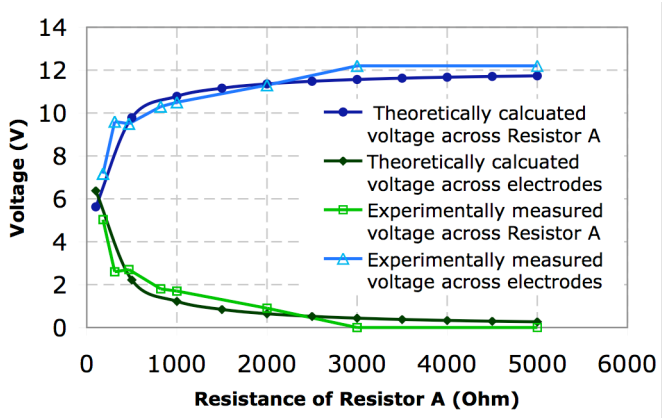

Figure 3. Theoretically calculated and experimentally measured voltages across both electrodes and Resistor A after formation of a nanowire when different values of resistor was used in the circuit.

THEORY

A. *Dielectrophoresis (DEP)*

Dielectrophoresis is defined as the lateral motion generated on uncharged particles due to polarization induced by non-uniform electric fields [7]. The Dielectrophoresis (DEP) force exerted on sperical particle can be expressed as:

$$< F_{DEP}(t) >= 2\pi\varepsilon_m a^3 \,\mathrm{Re}[K(\omega)]\nabla \mid E_{rms} \mid^2 \quad (1)$$

where ε_m is the dielectric permittivity of the medium, a is the radius of the particle, ω is the angular frequency, E_{rms} is the RMS of electric field intensity, and K is the Clausius-Mossoti factors which given by

$$K(w) \equiv \frac{\varepsilon^*_p - \varepsilon^*_m}{\varepsilon^*_p + 2\varepsilon^*_m} \quad (2)$$

where ε_p^* and ε_m^* are the complex permittivity of the particle and the medium respectively. The complex permittivity is given by:

$$\varepsilon^* = \varepsilon - j\frac{\sigma}{\omega} \quad (3)$$

where σ is the conductivities of medium [8].

The magnitudes of freqency, voltage, phyisical dimensions of the particles and real part of Clausius–Mossotti (CM) factor, govern the dielectrophoresis force. For spherical particles, the real part of CM factor can vary between –0.5 and +1.0. Particles move towards strong field region when the factor is positive and experience positive DEP force. The opposite situation occurs for negative DEP [2].

B. *Double Layer*

Double layer induced by electrostatic potential attracts ions of opposite charge from solution and repels ions with like charge. The circuit diagram in Fig.4 can approximately explain the behavior of double layer in electrode-electrode system. The potential drop across the double layer can be derived as [8]:

$$\Delta\phi_{DL} = \frac{\phi_o}{2 + i\omega\pi(\varepsilon_m/\sigma)\kappa x} \quad (4)$$

where ϕ_o is the applied potential, x is the distance from the electrode edge, κ is the reciprocal of the Debye length, which is a function of ionic strength of solution. The equation shows that potential drop across the double layer strongly dependent on the frequency of applied field and conductivities of medium (refer to Fig.5). In our experiment, gold colloidal are suspended in water. Conductivity of water varies from 0.05 Sm^{-1} to 0.00005 Sm^{-1}.

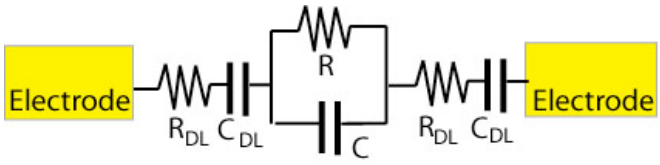

Figure 4. Approximate circuit diagram represent the double layer feature in an electrode-electrode system, where the double layer impendence can be represented as resistor R_{DL} and capacitor C_{DL} connected in series and the electrolyte impedence can be represented as resistor R and capacitor C connected in parallel [8].

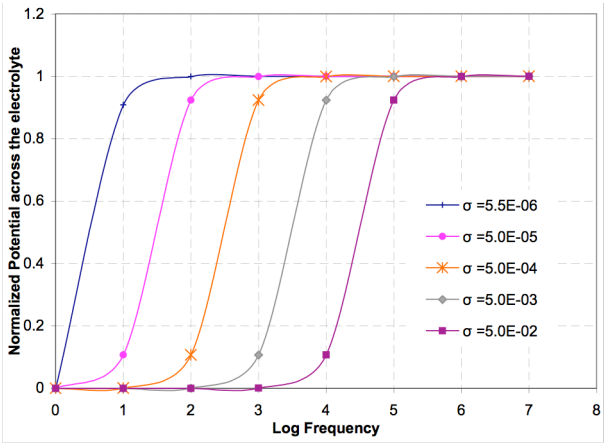

Figure 5. Real part of the normalized potential across electrolyte (outside double layer) as a function of frequency at different medium conductivities. This plot is calculated for gold colloidal suspended in water with ionic strength 0.0006 mol dm^{-3} at 25°C. Here, $\varepsilon_m=80\varepsilon_o$ and V_o=6V.

C. AC electroosmosis

The charges in the double layer between the surface and the electrolyte experience a force when an electric field is applied tangential to a surface bathed in electrolyte. Consequently movement of double layer charges pull the fluid along the surface and generate a flow [8]. The time average fluid velocity is given by:

$$v_{ac.omosis} = \frac{1}{8}\frac{\varepsilon_m \phi_o^2 \Omega^2}{\eta x(1+\Omega^2)^2} \tag{5}$$

where ϕ_o is the applied potential, η is the viscosity of medium and

$$\Omega = \frac{1}{2}\pi\kappa x(\varepsilon_m/\sigma)\omega \tag{6}$$

The equation shows that the time average fluid velocity strongly depends on both the frequency of applied electric field and the conductivity of solution (refer to Fig.6).

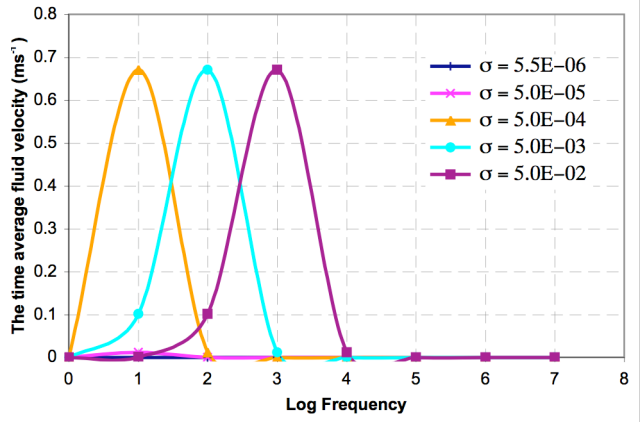

Figure 6. The time averaged fluid velocity by AC electroomosis at the middle of electrode gap as a function of frequency at different medium conductivities. This plot is calculated for gold colloidal suspended in water with ionic strength 0.0006 mol dm^{-3} at 25°C.

D. Electrothermal Fluid Flow

A large power density is generated in the fluid surrounding the electrode when high electric field is used to manipulate small particles [10]. When the conductivity of the medium is high, the power generated per unit volume increases. The ratio of electrothermal fluid velocity of the low to high frequency is approximately 10:1 [8]. The electrothermal body force on the fluid is given by:

$$< f_e >= \frac{2}{\pi^3 k}\frac{\sigma V_{rms}^4}{r^2}\prod(1-\frac{2\theta}{\pi})\hat{\theta} \tag{7}$$

where

$$\prod = \left[\frac{\alpha-\beta}{1+(\omega\tau_q)^2}-\frac{\alpha}{2}\right] \tag{8}$$

where V_{rms},is the RMS of applied potential, k is thermal conductivity of the medium, $\alpha = (1/\varepsilon)(\partial\varepsilon/\partial T)$, $\beta = (1/\sigma)(\partial\sigma/\partial T)$ and τ_q is the charge relaxation time (ε/σ). θ and r are given in Fig.7.

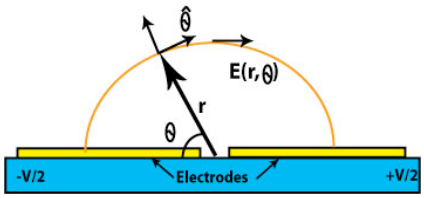

Figure 7. Definition of the parameters θ and r in the electrothermal body force equation [10].

An order of magnitude for a typical fluid flow velocity can be calculated by:

$$|u| = |f_e|\frac{l_o^2}{\eta} \tag{9}$$

where l_o is the characteristic distance of microelectrode [8]. Calculation on the order of magnitude of the maximum fluid velocity (θ equal to 0 or π) generated by joule heating under different assumed conductivity of the solution is shown in Table I.

TABLE I. CALCULATION ON THE ORDER OF MAGNITUDE OF THE MAXIMUM FLUID FLOW VELOCITY GENERATED BY ELECTROTHERMAL BODY FORCE.

Solvent Conductivity (Sm^{-1})	**Charge Relaxation frequency τ_q (s^{-1})**	**Order of magnitude of the fluid flow velocity generated by electrothermal body force (Note: "-" indicates movement away from electrodes)**	
		Frequency < τ_q	*Frequency* > τ_q
5.5×10^{-6}	7.76×10^{3}	-10^{-5}	10^{-6}
5.0×10^{-5}	7.06×10^{4}	-10^{-4}	10^{-5}
5.0×10^{-4}	7.06×10^{5}	-10^{-3}	10^{-4}
5.0×10^{-3}	7.06×10^{6}	-10^{-2}	10^{-3}
5.0×10^{-2}	7.06×10^{7}	-10^{-1}	10^{-2}

(Assumed V_{rms}= 8.487, $\varepsilon_m=80\varepsilon$, $l_o=2\mu m$ and $\eta=0.00089$ Pa•s. For water, α = -0.4% per degree and β =+2% per degree.)

EXPERIMENTAL RESULT

A. *Formation of Au nanowire by DEP force*

According to the theories of DEP, the real part of CM factor determines the direction of dipole. Particles move towards strong field region when the factor is positive and positive DEP force is induced (Fig.8). The opposite situation occurs for negative DEP. Comparing the normalized experimental PCF rate of 100 nm Au NPs under 12 V_{pk-pk} with the theoretical calculation of the Clausius-Mossotti (CM) factor using the single shell model sphere for gold colloidal particles suspended in D.I. water (Fig.9), it is apparent that DEP force dominates when frequency is higher than 10kHz. For frequencies below 10kHz, electrolysis and electroosmosis effects dominate, which prohibit PCF of NPs.

For the frequency ranges with negative CM factor (refer to Fig.9), no pearl chain formation was observed (except for range greater than 10^5 Hz) since particles experienced negative DEP force and were repelled from the electrodes. Distributions of gold particles were not uniform and steady because of fluid flow driven by other effects, e.g., AC electroomosis and electrothermal effect. From low to high frequencies, the dominant fluid flow shifts from the AC electroomotic flow to an electrothermally induced fluid flow, since electrothermal flow occurs in all frequencies and the magnitude of the AC electroomotic flow decreases when frequency increases. Further studies on dominant forces under various frequency range is explained in next section.

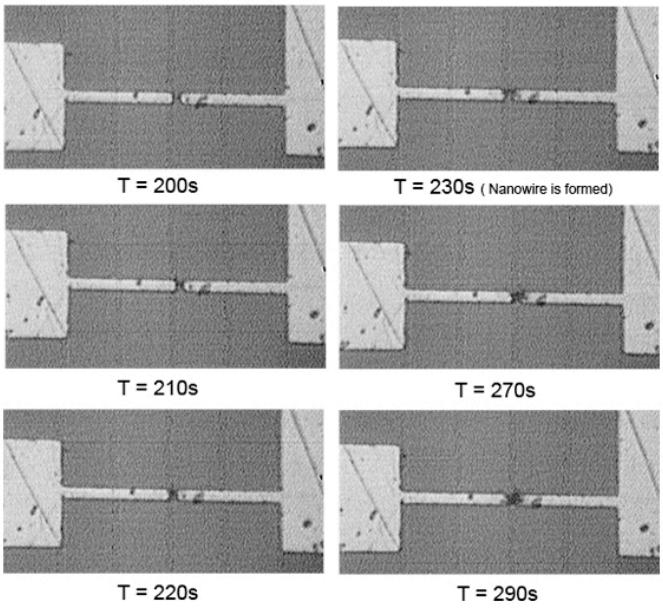

Figure 8. Experimental result of PCF under positive DEP force.

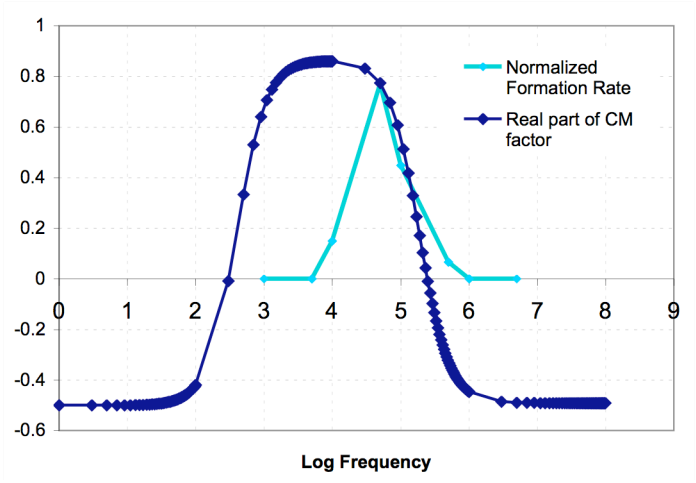

Figure 9. Comparsion of the experimental PCF rate of 100 nm under $12V_{pk-pk}$ voltages as a function of frequency with the theoretical calculation of the Clausius-Mossotti (CM) factor for 100nm single shell model sphere.

B. *Analyzing the observation of nanowire formation under various frequency range*

1) *10Hz to 100Hz*

Formation of bubbles caused by AC electrolysis prohibits the nanowire formation. During AC electrolysis, hydrogen and oxygen gas bubbles are generated due to electrolysis of water. The minimum voltage input for electrolysis of water can be determined by Nernst equation as 1.23V for DI water. Actual voltage is higher, which depends on the ion concentration and electrode gap distance. In our experiment, bubbles started to form at $2.3V_{rms}$ under 25Hz frequency. The rate of bubble growth increased along with the applied voltage. The amount of bubbles generated decreased when frequency increased, as redox reaction is limited by high frequency AC signal.

2) *100Hz to 10kHz*

DEP force is created only when frequency is greater than 10kHz, as shown by Morgan et al., [10], therefore, no pearl chain formation was observed in this frequency range. Besides the presence of dielectrophoresis effect, AC electroosomsis and double layer effects dominate under low frequency input. Fluid flow driven by electroomosis increased with the conductivity of the medium (refer to Fig. 6). For example, the magnitude of fluid velocity generated by the AC electroomosis effect is at least 10 times higher than the velocity generated by the DEP force, with the medium conductivity of 0.05-0.0005 Sm^{-1}. The velocities generated by DEP force for 10nm and 100nm Au NPs were calculated to be in the order of 10^{-4} and 10^{-2}, respectively [9]. Besides the electroomosis effect, most of the potential was drawn by the double layer under this frequency range (refer to Fig. 5), which accordingly decreases the magnitude of DEP force.

3) 10kHz for 10nm Au NPs

Fig. 10 shows that the pearl chain was formed away from the inter-electrode gap. According to the theory of electrothermal body force, the flow direction of the medium is determined by the charge relaxation frequency of the suspending medium. When the frequency of applied signal is smaller than relaxation frequency, $\prod$ factor is negative (refer to (8)), fluid flows away from the inter-electrode gap and vice-versa [11]. According to Table I, the charge relaxation frequency is around 10kHz when the medium conductivity is between 5.5×10^{-6} to 5.0×10^{-5} Sm^{-1}. Through the above analysis, we could consider that the conductivity of solvent is higher than that of DI-water (5.5×10^{-6} Sm^{-1}). This should be relevant to the actual conductivity of colloidal solution since the manufacturer claimed that chemical residual is left from manufacturing and chloride ion is presented in the colloidal solution.

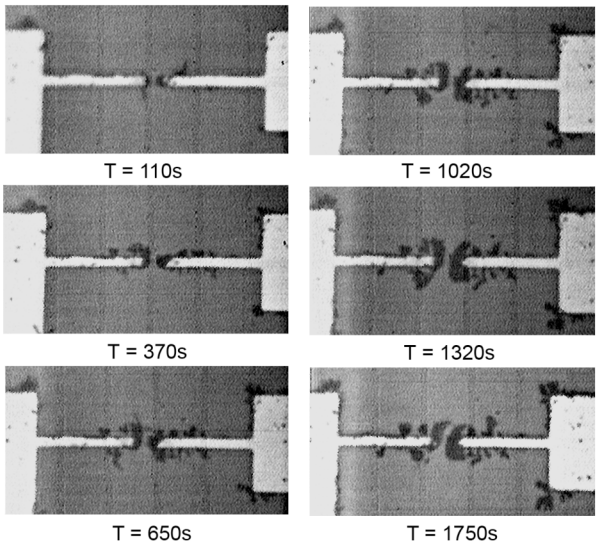

Figure 10. Experimental result of PCF under negative DEP force in which PC forms towards weak E-field region.

4) 10kHz to 5MHz for 100nm Au NPs
10kHz to 10MHz for 10nm Au NPs

In these cases, pearl chain formation was observed, which means that the positive DEP force dominanted, and particles were attracted to high E-field region. Variations in formation rate were detected when the applied voltage and the particle size varied. Fig. 11 shows that with high voltage, pearl chain began to form at higher frequency and the formation time decreased. This could be explained by the DEP force equation (refer to (1)) since $<F_{DEP}>$ is proportional to ∇E_{rms}^2.

Fig. 12 shows that the optimum frequency for formation shifted to higher frequency region when the particle size decreased. This could be explained by the DEP force equation of single shell model [9]. Theoretical calculation of DEP force shows that the velocity of 100nm particles is 100 times faster than 10nm. However, in most cases, our experimental results show that 10nm particles form faster or about the same time as those of 100nm. Further investigation on this issue is in progress.

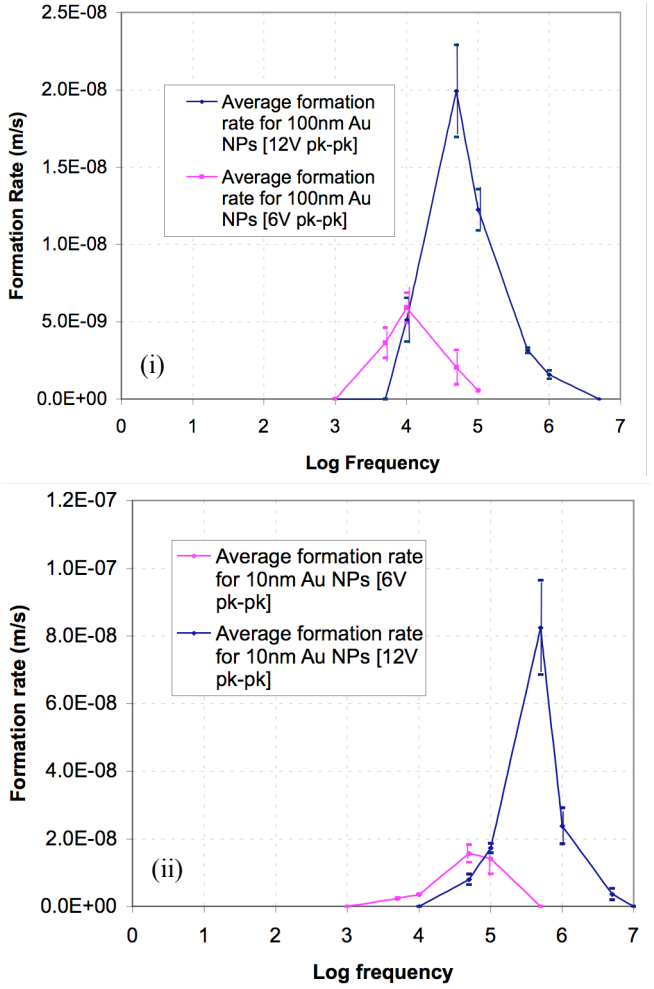

Figure 11. Experimental results on PCF rate of (i) 100 nm under 6 V_{pk-pk} and 12 V_{pk-pk}; (ii) 10 nm under 6 V_{pk-pk} and V_{pk-pk}.

CONCLUSION

A systematic experimental study of the PCF Au NPs together with a theoretical analysis of the dominant force during DEP manipulation was presented. At low frequency level, the solution fluid moved rapidly due to the AC electroomosis effect. Meanwhile, the applied voltage potential dropped across the double layer, hence pearl chain formations cannot be observed. Increasing the frequency of applied electric field, the magnitude of the AC electroosmotic flow decreased significantly and DEP force dominanted, and hence, PCF was observed. At high frequency level, particles experienced negative DEP force and were repelled from electrodes. Moreover, electrothermal body force generates fluid flow, and therefore, no PCF was observed in our experiments.

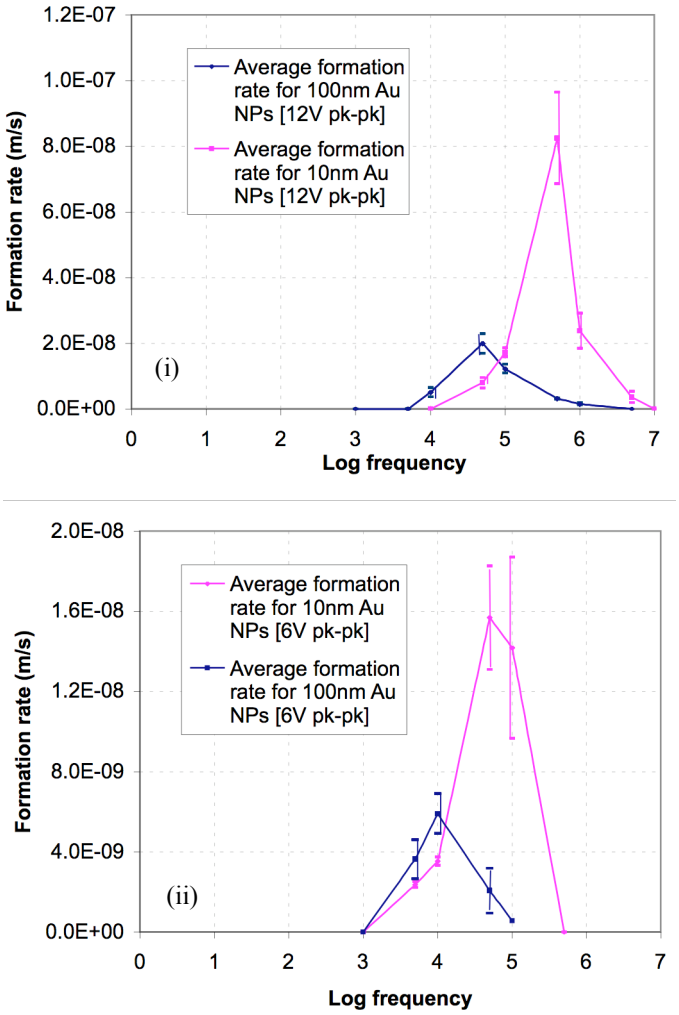

Fig. 12. Experimental results on PCF rate of (i) 10 nm and 100nm under 12 $V_{pk\text{-}pk}$ (ii) 10 nm and 100nm under 6 $V_{pk\text{-}pk}$.

ACKNOWLEDGMENT

The authors acknowledge all the members at the Centre for Micro and Nano Systems (CMNS) for their support and encouragement. In particular, the authors would like to thank Dr. Yan Li Qu, Ms. Mandy L. Y Sin, Mr. Gary C. T. Chow and Ms Winnie W. Y. Chow for their help in the electrode fabrication and useful discussions.

REFERENCES

[1] R. G. Grainger, "Intravascular contrast media—the past, the present, and the future", *Br. J. Radiol.*, vol. 55, no. 1, 1982.

[2] Lifeng Zheng, Shengdong Li, and Peter J. Burke, "Self-Assembled Gold Nanowire from Nanoparticles: An Electronic Route Towards DNA Nanosensors", *Nanoengineering: Fabrication, Properties, Optics and Devices,* SPIE vol. 5515, 2004.

[3] Gong Wai Leung, Fong Ting Lau, Siu Ling Leung, and Wen J. Li, "Formation of Au Colloidal Crystals for Optical Sensing by DEP-Based Nano-Assembly", *The 2nd IEEE Conference on Nano/Micro Engineered and Molecular Systems,* January 16, 2007.

[4] S. I. Khondaker, "Fabrication of nanoscale device using individual colloidal gold nanoparticles", *IEE Proc-Circuits Devices Syst.*, vol. 151, no.5, 2004.

[5] R. S. Wagner and W. C. Ellis, "Vapor-Liquid-Solid Mechanism of Single Crystal Growth", *Applied Physics Letters,* Vol.4, No.5, 1964.

[6] Birol Ozturk, Bret N. Flanders, Daniel R. Grischkowsk and Tetsuya D. Mishima, "Single-step growth and low resistance interconnecting of gold nanowire", *Nanotechnology, 18, 2007.*

[7] Pohl H. A., "Dielectrophoresis", *Cambridge: Cambridge University Press,* 1978.

[8] H. Morgan and N. G. Green, "AC Electrokinetics Colloidal and Nanoparticles", *Research Studies Press Ltd., 2003.*

[9] Minglin Li, Fei Fei, Yanli Qu, Zaili Dong, Wen J. Li, and Yuechao Wang, "Theoretical Analysis Based on Particle Electro-Mechanics for Au Pearl Chain Formation," *The 7th IEEE International Conference on Nanotechnology*, August 03, 2007.

[10] A. Ramos, H. Morgan, N. G. Green and A. Castellanos, "AC Electrokinetics: a review of forces in microelectrode structures", *J. Phys. D: Appl. Phys 31, 1998.*

[11] H. Morgan, N. G. Green, M. P. Hughes, W. Monagham, and T. C. Tan, "Large-area traveling-wave dielectrophoresis particle separator", *J. Micromech. Microeng.,* **7**, 65, 1997

[12] J. Clendenin, H. Rokadia, S. Tung and K. Ogburia, "Application of aligned carbon nanotubes in micro shear stress sensing", *The International Mechanical Engineering Congress and RD&D Expo*, IMECE2004-61227, November 13-19, 2004.